

## Chapter 36

# Construction and 100 h of operational experience of a 10-kW chemical looping combustor

Anders Lyngfelt and Hilmer Thunman

Dept. of Energy Conversion, Chalmers University of Technology

Chalmers University of Technology, 412 96 Göteborg, Sweden

### Abstract

Chemical-looping combustion is a new technology for burning gaseous fuels, with inherent separation of CO<sub>2</sub>. Metal oxide particles are used for the transfer of oxygen from the combustion air to the fuel, thus the combustion products CO<sub>2</sub> and H<sub>2</sub>O are obtained in a separate stream.

A 10 kW prototype for chemical-looping combustion has been designed, built and run with nickel-based oxygen-carrier particles. A total operation time of more than 100 h was accomplished with the same batch of particles, i.e. without adding fresh, unused material.

A high conversion of the fuel was reached, with approximately 0.5% CO, 1% H<sub>2</sub> and 0.1% methane in the exit stream, corresponding to a fuel conversion efficiency of 99.5% based on fuel heating value. The best way to treat the unconverted fuel is not clear, although it is believed that it can be separated from the liquefied CO<sub>2</sub> at a reasonable cost and recycled to the process.

There was no detectable leakage between the two reactor systems. Firstly, no CO<sub>2</sub> escapes from the system via the air reactor. Thus, 100% of the CO<sub>2</sub> is captured in the process. Secondly it should be possible to achieve an almost pure stream of CO<sub>2</sub> from the fuel reactor, with the possible exception of unconverted fuel, or inert compounds associated with the fuel, e.g. N<sub>2</sub>.

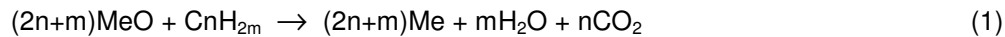
No decrease in reactivity or particle strength was seen during the test period. The loss of fines was small

and decreased continuously during the test period. In the end of the period the loss of fines, i.e. particles smaller than 45  $\mu\text{m}$  was 0.0023% per hour. If this can be assumed to be a relevant measure of the steady-state attrition, it corresponds to a lifetime of the particles of 40 000 h. Assuming a lifetime of the particles one order of magnitude lower, i.e. 4000 h, the cost of particles in the process is estimated to be below 1 €/ton of CO<sub>2</sub> captured.

## Introduction

### Chemical-looping combustion

Chemical-looping combustion has been discussed earlier in the literature as an alternative to normal combustion. The system is composed of two reactors, an air and a fuel reactor, as shown in Figure 1. The fuel needs to be in a gaseous form and is introduced to the fuel reactor, which contains a metal oxide, MeO. The fuel and the metal oxide react according to:



The exit gas stream from the fuel reactor contains CO<sub>2</sub> and H<sub>2</sub>O, and almost pure CO<sub>2</sub> is obtained when H<sub>2</sub>O is condensed. The reduced metal oxide, Me, is transferred to the air reactor where the metal is oxidized according to:



[Figure 1]

The air which oxidizes the metal produces a flue gas containing only N<sub>2</sub> and some unused O<sub>2</sub>. Depending upon the metal oxide used, reaction (1) is often endothermic, while reaction (2) is exothermic. The total amount of heat evolved from reaction (1) and (2) is the same as for normal combustion, where the oxygen is in direct contact with the fuel. The advantage of chemical-looping combustion compared to normal combustion is that CO<sub>2</sub> is not diluted with N<sub>2</sub> but obtained in a relatively pure form without any energy needed for separation.

Originally, the process was proposed as a method to enhance the thermal efficiency of fuel combustion, [1]. The idea was to supply low-temperature heat to the endothermic reaction in the fuel reactor, thereby increasing the amount of heat produced in the high-temperature air reactor. This possibility is not considered in the present application, since it would make the process more complex and also involves extra demands on the properties of the oxygen carrier.

The reactors in Figure 1 could be designed in a variety of ways, but two interconnected fluidized beds have an advantage over alternative designs, because the process requires a good contact between gas and solids as well as a significant flow of solid material between the two reactors, [2]. Such a circulating system composed of two connected fluidized beds, a high velocity riser and a low velocity bubbling fluidized bed, is shown in Figure 2. The bed material circulating between the two fluidized beds is the oxygen-carrier in the form of metal oxide particles. In the air reactor, or the riser, oxygen is transferred from the combustion air to the oxygen carrier. In the low velocity fluidized bed, or the fuel reactor, oxygen is transferred from the oxygen carrier to the fuel. The volumetric gas flow in the air reactor is approximately ten times larger than that of the gaseous fuel, and to keep a reasonable size of the reactor a high velocity is advisable in the air reactor.

[Figure 2]

The gas velocity in the riser provides the driving force for the circulation of particles between the two beds. Thus, the particles carried away from the riser are recovered by a cyclone and led to the fuel reactor. From the fuel reactor the particles are returned to the air reactor by means of gravity; the fuel reactor bed is at a higher level than the bed of the air reactor. After condensation of the water, the remaining gas, containing mostly CO<sub>2</sub>, is compressed and cooled in stages to yield liquid CO<sub>2</sub>. If there is remaining non-condensable gas from this stream containing unreacted combustibles, one option would be to recover this gas and recycle it to the fuel reactor. Small amounts of water left in the liquid CO<sub>2</sub> have to be removed by a regenerable solvent to make the CO<sub>2</sub> flow less corrosive.

A number of publications related to the development of oxygen-carrier particles have been issued by the research groups at Tokyo Institute of Technology [3-13], Chalmers University of Technology [14-20], Korea Institute of Energy Research [21-26], TDA Inc [27-29], CSIC-ICB in Zaragoza [30], National Institute for Resources and Environment in Japan [31] and Politecnico di Milano[32]. Also a number of papers investigate the possible thermal efficiencies of the power processes involving chemical-looping combustion. However, there seem to be no literature data showing successful operation of a chemical-looping combustor for any longer periods. The only data available is from a small laboratory unit using hydrogen, mixed with 33% argon, as fuel [13]. The system consisted of two interconnected columns in an

oven, and seems to have no particle locks. The principles of the circulation system are not reported and since the two exiting gas streams were mixed before gas analysis it is not possible to judge if there was any gas mixing between the two reactors. The authors performed tests at 600, 900 and 1200 C with complete conversion at the two higher temperatures. Gas conversion data are presented for a 5-hour test at 1200 C. The particles were made of a mixture of NiO and Al<sub>2</sub>O<sub>3</sub>, and it is interesting to note the high temperature used.

Continuous testing in a chemical-looping prototype is not only needed to demonstrate the principle of this new combustion technology. It is also essential to verify the usefulness of the particles developed. Most laboratory tests of particle reactivity cover only a limited number of cycles. The number of hours of operation for the particles in a real system could be in the order of 1000 or more, whereas the number of cycles for a particles could be in the order of 100 000. Furthermore the laboratory tests do not show if the particles would be degraded by attrition or fragmentation at the velocities in a full-scale unit.

The purpose of the present project was to demonstrate this new combustion technology and to verify that the oxygen-carrier particles developed are able to survive the conditions of a real process.

## Experimental

### Design of a 10 kW chemical-looping combustion (CLC) prototype

The 10 kW prototype was not designed primarily to be a small model of a full-scale unit, but the major priority was to obtain a unit that works, that is flexible and can be used to study particles and reactions in continuous operation. Flexibility is important to accommodate for the uncertainty regarding properties of the particles best suited for the process. Flexibility is also important to allow for parameter variations in testing. Lastly, flexibility is important as there are inevitable uncertainties in the design.

The cross-section area of the air reactor is determined by the need to have the right particle circulation flow. Above the air reactor there is a conical section where the particle-containing gas enters the riser. In order to reduce heat losses a small diameter of the riser is an advantage. The diameter of the riser was chosen to give the velocities expected in a larger commercial plant.

Also the cross-section of the fuel reactor was determined by the possible gas velocities in the bed. The upper velocity limit in the fuel reactor is given by elutriation. The lower limit is related to the minimum fluidization velocity, which has to be exceeded to achieve proper fluidization of the bed. In order to accommodate for the gas volume expansion in the fuel reactor, the cross-section area increases with height by means of two conical sections.

Several factors affect the choice of air reactor height. Based on estimated reactivity of most metal oxide particles the needed height of the dense bed is small. In order to achieve stable operation conditions in this small unit without systems for control of particle inventory, a higher bed may be needed. In the height of the air reactor the adequate surface area for cooling was also considered. Thus, the air reactor height was chosen to consider particle reactivity, stability of operation and need for cooling.

The bed height of the fuel reactor was chosen based on the reactivities obtained in previous studies with iron-based oxygen carriers. The bed height is controlled by an overflow exit. To the total height of the fuel reactor was added a freeboard with sufficient height and a margin for varying the bed height. The bed

height can be varied by changing the height of the overflow. In order to do this, however, the insulation has to be removed and the fuel reactor opened.

The diameters of the downcomers were chosen to be sufficient for the expected circulation flows. Ideally the particle column height in the standpipes leading into the particle locks will correspond to the pressure difference over the particle lock. However, this column height should also accommodate for the friction of the particle flow through the particle lock as well as variations in pressure difference and particle flow.

The total pressure difference to be accommodated by heights of the particle columns in the two downcomers is given by the pressure drop in the riser and the inlet of the cyclone. To accommodate for variations in pressure difference under varying operation conditions a significant margin was added to this.

For particle locks the pot seal type was chosen. The cyclone was dimensioned for a gas flow corresponding to a thermal power of 10 kW and an air ratio of two. A conventional cyclone was chosen.

The dimensioning of the unit was made together with University of Vienna, where it was tested in a cold flow model, see Kronberger et al. (Chapter 30 in this publication). The results from the cold flow model followed the expectations and only minor modifications were made when the hot unit was built.

### **Fuel properties**

Natural gas with the composition shown in Table 1 was used. The purpose of the project was to develop chemical-looping for application in a refinery, i.e. to burn refinery gas. Table 1 shows a comparison of refinery gas and natural gas. The major difference is a larger content of hydrogen and hydrocarbons with 2 to 4 carbon atoms. The properties, e.g. fuel heating value and volume expansion, of the two fuels are rather similar, although the refinery gas can be expected to be more reactive because of the higher hydrogen content.

[Table 1]

### **Construction and test of CLC.**

The reactor system is shown in Figure 3 together with parts of the external system needed for operation

and data collection. The external system includes:

- Free-convection air-cooling of exiting streams in two 8-m long finned tubes,
- System for accommodating the thermal expansion of the reactor system and the cooling tubes, including scaffold, suspension springs and bellows.
- Two filters for the capture of particles elutriated from the air reactor. The filters were large to achieve low pressure drop. It is possible to switch from one filter to the other during operation in order to enable measurement of elutriation over a chosen time period
- A water seal to control the pressure balance of the reactors, i.e. air reactor and cyclone vs. fuel reactor. The water seal has an overflow exit and also acts as a condensate trap for the humid gas from the fuel reactor. The water seal also collects the elutriated particles from the fuel reactor. For this reason distilled water was used in the water seal.
- Connection to chimney.
- 15 kW preheater that is able to preheat the process air flow up to 1040 C.
- 50 V transformer for supply of direct current to preheater, and control of outlet temperature.
- Thermal insulation of reactor system.
- System for gas analysis, including two gas analysers for CO, CO<sub>2</sub> and O<sub>2</sub>, two gas analysers for CH<sub>4</sub>, connection of gas analysers, gas pre-treatment of the two exit streams, system for calibration and data collection.
- 26 pressure taps and connection of those to pressure transducers and gas purging, calibration and system for data collection.
- 6 thermocouples for temperature measurements and connection of those to the data collection system.
- Gas supply system, including fuel for the process located in a separate building outside the workshop, inert gas for both particle locks, inert gas for fuel reactor, combustion air, cooling air, and also the possibility to run air instead of inert gas to reduce the cost of gas when fuel is not added.
- Mass flow controllers for six gas flows, i.e. combustion air, cooling air, fuel, inert gas to fuel reactor, gas to upper particle lock, gas to lower particle lock. Data collection of these gas flows.
- Automatic temperature control of air reactor by cooling air which is led fed to a cooling jacket surrounding the air reactor, making it possible to keep air reactor temperature  $\pm 1-2$  C.



- Monitoring system with displays allowing immediate survey of *i)* five important pressure drops - over lower particle lock, higher particle lock, riser, air reactor bed and fuel reactor bed, *ii)* air and fuel reactor temperature, *iii)* all gas concentrations and *iv)* all gas flows.

- System for additional start-up heating through methane addition to the air reactor.

[Figure 3]

## **Results and Discussion**

### **Initial tests**

Initial test runs with sand were made to gain experience on how to run the system and to find weak points that need improvement. In connection with these sand tests the gas leakage between the two reactors, i.e. the fuel and air reactors, was studied. This was made by measuring the oxygen concentration in the off-gas when varying the gas added, i.e. nitrogen or air, to the particle locks, air reactor and fuel reactor. These tests indicate that gas leakage between the reactors is below the detection limit with the analysers used, i.e. the dilution of the gas from the fuel reactor is less than 0.5%.

### **Overview of operation in chemical-looping mode**

A total of more than 100 hours of continuous running of the 10 kW chemical-looping combustor prototype with nickel-based particles has been accomplished in August and September, 2003. The tests were made during four weeks of running and involve 12 days of running in CLC operation, typically from 11 am to 9 pm. An overview of the testing days is given in Table 2.

[Table 2]

In the morning gas analysers were calibrated. The electrical preheating was not sufficient to reach the temperature of operation and therefore it was necessary to raise the temperature by burning fuel in the air reactor. During the nights the fuel was switched off and the unit was run with electrical preheating, and this was continued until operation was resumed on the following day. In addition to the actual CLC operation, the particles have therefore been in circulation at high temperature during the night and the morning. The total time of circulation of the particles is almost 300 h.

Almost full conversion of the fuel was accomplished. No CO<sub>2</sub> was found in the gas from the air reactor. Operation was very stable, i.e. the process could often be run until the fuel addition was stopped for the night without any modifications of the operation, such as adjustments of gas flows. A number of technical problems, such as gas and particle leakages, thermocouple failure, plugging of pressure taps etc. were encountered during operation causing delays. During operation only two things had to be addressed that which were related to the actual CLC process:

i) In the first day, during the first two hours of operation, the fluidization velocity of the particle locks was not sufficient, which resulted in a stop of particle circulation on a few occasions. After increasing the gas flow to the particle locks, no stop in circulation occurred during the rest of the test period. To avoid any risk of particles gathering in the cyclone, the gas flow to the upper lock was always higher to make sure that any stop in circulation would be likely to occur in the lower particle lock.

ii) After an extended time of operation the loss of smaller particles resulted in poorer circulation, giving lower temperature in the fuel reactor. Thus, the flow/velocity in the air reactor had to be increased to achieve sufficient circulation, i.e. sufficient temperature in the fuel reactor. After some days of operation addition of previously elutriated particles was made. Thus, elutriated particles were recycled twice during the test period, i.e. on day six and day ten of the twelve days of operation.

### **Gas concentrations**

The equilibrium concentrations of CO and H<sub>2</sub> over NiO for a methane flue gas (66.7% H<sub>2</sub>O and 33.3% CO<sub>2</sub>), are shown in Table 3. After condensation of H<sub>2</sub>O the concentration will be three times higher in the CO<sub>2</sub> stream. In the prototype tests there is also a dilution of the gas with the inert gas used to fluidize the particle locks, typically the concentration is reduced by 20-30% depending on the flows. In a real system the flows to the particle locks would be smaller in relation to the fuel flow and most likely steam would be used as fluidization gas, thus avoiding any dilution of the CO<sub>2</sub> produced.

[Table 3]

The measured concentration is close to equilibrium for CO. A typical value is 0.55% CO and the equilibrium concentration, if corrected for dilution and condensation is about 0.50. H<sub>2</sub> was not measured on line, but bag samples were taken and sent for analysis. These showed that the H<sub>2</sub> concentration was

1%, which fits well with the values expected from the thermodynamic equilibrium data if the dilution with inert gas is considered, cf. Table 3.

The measured concentration of methane in the gas from the fuel reactor varied between 0.05 and 1%. The higher values were, quite unexpectedly, seen for higher temperatures in the fuel reactor. The temperature dependence was very clear. The equilibrium concentration of methane is below  $10^{-6}$  ppm in this temperature range, i.e. zero for all practical purposes. Furthermore, it would be expected that higher temperatures would increase the reaction rates and thus improve the conversion. However, the temperature dependence of methane is most likely an artefact. The temperature in the fuel reactor is correlated to the recirculation of particles and it is believed that the methane concentration increases when the circulation increases.

It is known from the laboratory testing that Ni-based oxygen carriers during reduction, show a small initial peak of methane of approximately 1%. This peak disappears rapidly as the conversion of the NiO to Ni proceeds. No such peak has been seen for other metal oxides. Ni is a known catalyst for the reaction between  $\text{CH}_4$  and  $\text{H}_2\text{O}$  and it is believed that the peak is a result of the beneficial catalytic effect of the reaction product, most likely in promoting intermediary reactions. Thus, it is believed that an increased circulation reduces the presence of Ni so much that methane conversion is decreased.

A possible implication of this observation for the full-scale application could be that lower circulation, and thus lower fuel reactor temperature, is advantageous. However, it should be pointed out that in a small unit such as the prototype the relative heat losses from the fuel reactor are larger than in a full-scale unit, resulting in the need for a higher recirculation. Furthermore, it is not unlikely that this effect could be offset by adapting a much lower residence time in the air reactor, thus circulating a not totally oxidized metal oxide. This would be difficult to test in a small unit where operation would be too unstable for a system with only indirect control of the air reactor solids inventory. By indirect control is here meant the possibility of manual addition of particles.

### **Start-up and stop in operation**

A typical start-up of operation is shown in Figure 4. After heating the system to a suitable temperature, the start-up is simply made by shifting the incoming gas flow to the fuel reactor from nitrogen to methane. This is accomplished within a few seconds. At the start the measured concentrations of CO<sub>2</sub>, CO and methane increase as fast as the response times of the gas sampling lines and the gas analysers allow. CO peaks at 0.6% but reaches a steady-state value of approximately 0.5% within a few minutes. A pronounced transient is seen for CH<sub>4</sub> which has an initial peak of 1.5% but drops down to its steady state value of 0.1% within 5-10 minutes. Ni is a catalyst, as pointed out above, and this transient is believed to be associated with the increased presence of the reduction product, i.e. Ni, in the fuel reactor. Also for the oxygen there is a transient and steady-state conditions are reached after 10-15 minutes.

[Figure 4]

Stop of fuel is shown in Figure 5. The procedure involves switching from fuel to nitrogen, see the dashed vertical line to the left, and after a little more than three minutes nitrogen is substituted for oxygen, see the dashed two vertical lines on the right-hand side. The oxygen concentration increases rapidly and reaches a concentration of 20% within four minutes. The fluctuations in oxygen are associated with variations in the recirculation rate of particles. The CO, CH<sub>4</sub>, and CO<sub>2</sub> decrease to zero as fast as the response times of the gas paths, gas sampling lines and the gas analysers, allow. CO<sub>2</sub> reaches zero a little after CO and CH<sub>4</sub> because of its much higher starting value.

[Figure 5]

No increase in CO<sub>2</sub> or CO is seen after air addition to the fuel reactor is started. This indicates that there was no char formation in the fuel reactor. However, it can be noted that the oxygen level is very low after switching from inert gas to air, and increases slowly. After eight minutes it has only reached six percent. This is of course an effect of the oxidation of the particles in the fuel reactor.

### **Stop of circulation**

The effect of stopping the circulation on purpose is shown in Figure 6. The stop in circulation is accomplished by stopping the inert gas flow to the lower particle lock. Thus, this is defluidized and the

particle flow from the fuel reactor to the air reactor is immediately stopped. However, the flow from the air reactor to the fuel reactor will continue and decrease gradually. The stop in circulation is shown in the figure by the dashed vertical lines indicating stop and start of the gas flow to the lower particle lock. After a short delay caused by the residence time in the gas sampling lines, the oxygen rises very rapidly and reaches 20% in less than half a minute. The response in CO and CH<sub>4</sub> is slower. After approximately two minutes the CO starts a gradual increase, whereas the CH<sub>4</sub> falls to zero. The latter again supports the supposition that increased presence of Ni gives higher methane conversion. When the circulation is started again a very rapid response in oxygen is seen, and also the response in CO is reasonably rapid. The oxygen concentration after restarting the circulation is much lower than the steady-state value but increases gradually. The second stop is a little longer and produces a more dramatic increase in CO.

[Figure 6]

### **Stability of operation and change in particle size distribution**

The stability of operation during a longer period of operation, 11 hours, is illustrated by Figure 7. The only automated operational control is that of the air reactor temperature, which is kept constant by the external air cooler. The circulation is controlled manually by adjusting the set point flow of the air mass flow controller. As seen in the diagram there is a gradual decrease in the circulation which has the effect of lowering the fuel reactor temperature. This in turn means raised CO concentration. After six hours of operation the CO has increased from 0.5% to 1.5%, and then the air flow is increased by 7%. The circulation increases and the CO is immediately reduced. The CH<sub>4</sub> on the other hand falls as the circulation goes down and then rises when the circulation is increased. Again this is believed to be an effect of circulation and not of temperature.

[Figure 7]

The gradual decrease in circulation is an effect of a loss of particles from the system, which also means that the average size of the particles increases. As mentioned above this loss of particles is neutralized by recycling the elutriated particles, as was done on days 6 and 10. In a full-scale unit the cyclone would have better efficiency and elutriated particles would be recycled more regularly to maintain the solids inventory constant.

The particle circulation mass flow was estimated by two different methods. Unfortunately, these give rather different results. The variations, however, can be illustrated and are shown in Figure 7 and 10 by a circulation index which should be proportional to the actual circulation mass flow.

### **Effect of temperature**

The system has been run with fuel reactor temperatures between 750 and 900 C. Lower temperatures have occasionally been tested, e.g. a fuel reactor temperature of 560 C, but at this low temperature the conversion of methane was only 75%.

Figure 8 shows the CO concentration versus fuel reactor temperature. At about 790 C there is a minimum and below this CO increases markedly with lowered temperature. Above 790 C the CO concentration is very close to the equilibrium concentration as indicated by the dashed line. The equilibrium concentration shown is corrected for the dilution of inert gas.

[Figure 8]

Figure 9 shows CH<sub>4</sub> versus fuel reactor temperature. An attempt to separate the effect of circulation and of temperature was made by varying the temperature in the air reactor, i.e. the temperature of the incoming particles. The data suggest that a lower recirculation gives a lower CH<sub>4</sub> at the same temperature. In Figure 10 the CH<sub>4</sub> data for the same period are shown versus the circulation index. A clear correlation between circulation flow and CH<sub>4</sub> is seen. These data support the assumption that the circulation, and not the temperature, is the cause of the variation in CH<sub>4</sub>. However, to achieve conclusive evidence for this the system would have to be modified to allow a variation of the fuel reactor temperature which is independent of particle circulation.

[Figure 9], [Figure 10]

### **Loss of fines**

Attrition or fragmentation of particles leading to the production of fines is critical for the lifetime of the

particles. It is therefore essential to analyse the production of fines. The size distribution of material elutriated and caught in the filters is shown in Table 4. It is clear that the elutriation of fines decreases significantly with time. The high initial values are mainly associated with fines present in the added material, whereas the fine material elutriated in the later part of the process could be a result of attrition.

[Table 4]

In Figure 11 is shown the loss of fines versus time. Here the loss of fines is defined as the loss of particles smaller than 45  $\mu\text{m}$ . It is assumed that particles of this size will have a short residence time in a commercial unit and thus be of little use in the process, whereas it would be meaningful to recycle larger particles. The loss of fines includes particles elutriated from the air reactor, i.e. captured in the filter, and from the fuel reactor, i.e. captured in the water trap. For practical reasons the particles in the water trap were not collected daily, which explains the plateaus in the curve. It is clear that the loss of fines is rapidly decreasing with time during the whole test period. Two mechanisms can explain this decrease, that is *i*) fines present with starting material and *ii*) a gradual decrease in the attrition of particles, for instance because the material becomes harder or that irregularities are gradually worn off.

[Figure 11]

The latter is supported by photos of the particles, see Figs. 12 and 13. It can be seen that smaller spheres, "satellites", are sintered onto the larger spheres or together in groups. It is very likely that an important mechanism for production of fines is associated with these "satellites" being ripped from the larger particles. It is also clear from photos of particles elutriated later during the test series that the number of satellites has decreased, although satellites still remain after 100 h of operation.

[Figure 12,13]

After day three, when most of the fine material added with the original particles has been elutriated, there is a slower but seemingly exponential decrease in the particle loss. In this period the loss of fines is reduced to half every three days.

The loss of fines in the size fraction below 45  $\mu\text{m}$  is 0.0023%/hour at the end of the period, see Figure 11.

If this value can be taken as a measure of the lifetime of the particles, this leads to an approximate lifetime of the particles of 40 000 h. This indicates that the lifetime of these particles may be very long, provided that there is no chemical degradation. This would of course have to be verified by testing for longer periods.

An important question for the data on particle loss is the relevance of those data for large units. Attrition is related to the velocity in the riser and the velocity of the gas coming out of the air distributor nozzles in the bottom bed. The fluidization velocity in the air reactor was considerably lower compared to that expected in a large unit. However, because of the area decrease into the riser, the riser velocities during operation are similar to that expected in a full-scale unit. Furthermore the velocities from the inlet nozzles were very high during night operation without reaction, i.e. with preheating. This is because the pressure drop of the nozzles in the air reactor was dimensioned to give sufficient pressure drop during operation at various loads, i.e. with air that is not preheated. Thus, during the period of nearer 200 h when the reactor system was run without reaction, and the temperature was kept by preheated inlet air, the velocity of the gas entering the system was high, in the order of 100 m/s. This velocity is much higher than that expected from nozzles in a full-scale plant, and may be an important source for attrition during the tests in the prototype. In conclusion it is likely that the tests in the prototype do not underpredict the attrition in a full-scale unit.

Tests of particles in the laboratory after 100 h of operation indicate that there was no loss in reactivity or any decrease in the crushing strength of the particles.

### **Mass balance**

Table 5 shows a mass balance over the whole period in per cent of the originally added material. The total amount of material found in the filters was 73.1%. In addition to this 4.5% of material elutriated from the fuel reactor was caught in the water seal. The mass balance shows that 81.5% is totally lost from the system through elutriation and leaks and 32.3% was recycled during the period. Thus, it would be expected that 50.8% would remain in system if mass changes due to reactions are neglected, which is seen in the column with the heading: "initially added + recycled – lost". The amount actually found was



48.9%, i.e. 2% less than expected. A mass decrease of that order would be expected because the elutriated and remaining particles are not fully oxidized. Thus, it can be concluded that the mass balance is fulfilled.

[Table 5]

### **Tests with iron-based oxygen carrier**

A shorter test series with an iron-based oxygen-carrier was made just before the end of the project. During five days more than 17 h of operation with iron-based particles was accomplished. Operation was discontinued because of technical difficulties associated with the external system that were not possible to solve before the end of the project. Just as with the NiO, operation of the process with iron-based particles was simple; the important difference being that higher concentrations of CO and CH<sub>4</sub> were obtained, as a consequence of the lower reactivity of this oxygen-carrier.

The unit was operated with varying circulation flows, varying fuel flows and varying fuel reactor temperature. It was evident that both the CO and methane concentration in the exiting gas was a function of these parameters. In general, the conversion was highest for low fuel flow, high circulation and high fuel reactor temperature. The concentrations of CH<sub>4</sub> and CO were normally in the range 2 – 8%. However, the interpretation of the results was difficult because of inconsistencies that are not fully understood at present. The lowest concentrations obtained for CO and CH<sub>4</sub> were slightly below 2%. The test period, 17 h, was too short for any conclusions on the lifetime of the particles.

### **Particle development**

In parallel with the design and construction of the chemical-looping prototype, oxygen-carrier particles were developed and tested. The work was made in cooperation with CSIC, see Adané et al. (Chapter 29 in this publication). The particles produced at Chalmers were made by freeze-granulation and tested in a small fluidized bed. The results are summarized in Figure 14, where a rate index is shown versus crushing strength. The rate index is a measure of reactivity, cf. [19]. Also indicated is if the particles showed any tendency for agglomeration. As is seen many of the most reactive particles are often soft, or

have a tendency to agglomerate. The detailed results from this study will be published elsewhere, e.g. [29].

[Figure 14]

### **Cost of NiO-based particles**

With nickel being the most expensive of the raw materials used, the cost of raw material is assumed to be 3 €/kg. The cost of manufacture by spray-drying, sintering etc. is estimated to 0.5 €/kg, based on actual prices for material sold from a Swedish plant. Assuming a loss in sieving because of demands for a more narrow size range, the production cost is assumed to be 1 €/kg. This gives a total cost of 4 €/kg. If fine material lost from operation can be recycled this would reduce the cost significantly but not below the production cost.

The solids inventory in the prototype differs much from what is expected in a large unit. Firstly, the bed height of the fuel reactor was dimensioned for less reactive iron-based oxygen-carriers, and secondly the bed of the air reactor is much larger to achieve stable conditions in this small unit. Therefore no safe conclusions on needed solids inventory can be made from the tests. Here it is assumed that the solids inventory in a full-scale unit is in the order of 100-200 kg/MW.

The total cost of particles per ton of CO<sub>2</sub> captured is determined by three assumptions, particle inventory, lifetime and specific particle cost. Table 6 below summarizes the estimation of the particle cost. The numbers used for all three of the assumptions are conservative, see notes below the table. There has previously been a concern that the cost of the particles could be a show-stopper for this technology. With an estimated cost of the particles of the order of one €/ton of CO<sub>2</sub> captured, this is definitely not so.

[Table 6]

### **Conclusions**

A 10 kW prototype for chemical-looping combustion has been designed, built and run with nickel-based oxygen carrier particles. A total operation time of more than 100 h was reached with the same batch of particles, i.e. without adding fresh, unused material. The operation involves twelve days of operation,

with typically eight hours per day. During night-time and during start-up of operation the system was kept at high-temperature and circulation with electrical preheating. Thus, the actual time that the particles have been circulating in the system is close to 300 h.

A high conversion of the added methane was accomplished, with approximately 0.5% CO, 1% H<sub>2</sub> and 0.1% methane in the exit stream. The presence of CO and H<sub>2</sub> is a thermodynamic effect related to the NiO/Ni system, and means that the process is very close to equilibrium. The presence of these compounds corresponds to a fuel conversion efficiency of 99.5% based on fuel heating value. The best way to treat the unconverted fuel is not clear, although it is believed that it can be separated from the liquefied CO<sub>2</sub> at a reasonable cost and recycled to the process.

There was no detectable leakage between the two reactors. Firstly, no CO<sub>2</sub> escapes from the system via the air reactor. Thus, 100% of the CO<sub>2</sub> is captured in the process. Secondly, the leakage of gas from the air reactor to the fuel reactor was tested during initial testing with sand particles, and no leakage was found. Thus, the CO<sub>2</sub> leaving the fuel reactor should be pure, with the possible exception of unconverted fuel, or inert compounds associated with the fuel, e.g. N<sub>2</sub>.

No decrease in reactivity was seen during the test period. This was also verified by laboratory analyses of particles elutriated from the system at the end of the testing period. Furthermore analysis of crushing strength of these particles indicated that the particles were equally hard after 100 h of operation as the original particles.

The loss of fines was small and decreased continuously during the test period. In the end of the period the loss of fines, i.e. particles smaller than 45 µm was 0.0023% per hour. If this assumed to be a relevant measure of the steady-state attrition, it corresponds to a lifetime of the particles of 40 000 h. Assuming a lifetime of the particles one order of magnitude lower, i.e. 4000 h, the cost of particles in the process is estimated to be below 1 €/ton of CO<sub>2</sub> captured.

## **Recommendations**

Long-term tests with particles should be made in order to verify the expected long lifetime of the particles.

## Acknowledgements

This work was made in the EU financed research project Grangemouth Advanced CO<sub>2</sub> Capture Project (GRACE), ENK5-CT-2001-00571, led by British Petroleum and part of the CO<sub>2</sub> Capture Project (CCP).

## References

- [1] Richter HJ, Knoche KF. Reversibility of Combustion Process. American Chemical Society Symposium Series, Washington D.C., 1983. p. 71-85.
- [2] Lyngfelt A, Leckner B, Mattisson T. A fluidized-bed combustion process with inherent CO<sub>2</sub> separation; application of chemical-looping combustion. *Chemical Engineering Science* 2001;56:3101-3113.
- [3] Nakano Y, Iwamoto S, Maeda T, Ishida M, Akehata T. Characteristics of Reduction and Oxidation Cycle Process by Use of aFe<sub>2</sub>O<sub>3</sub> Medium. *Iron & Steel Journal of Japan* 1986;72:1521-1528.
- [4] Ishida M, Jin H. A Novel Combustion Based on Chemical-Looping Reactions and Its Reaction Kinetics. *Journal of Chemical Engineering of Japan* 1994;27(3):296-301.
- [5] Ishida M, Jin H. A Novel Chemical-Looping Combustor without NO<sub>x</sub> Formation. *Industrial and Engineering Chemistry Research* 1996;35:2469-2472.
- [6] Ishida M, Jin H, Okamoto T. A Fundamental Study of a New Kind of Medium Material for Chemical-Looping Combustion. *Energy & Fuels* 1996;10:958-963.
- [7] Ishida M, Jin H. CO<sub>2</sub> Recovery in a Power Plant with Chemical Looping Combustion. *Energy Conversion and Management* 1997;38:187-192.
- [8] Ishida M, Jin H, Okamoto T. Kinetic Behavior of Solid Particles in Chemical-Looping Combustion: Suppressing Carbon Deposition in Reduction. *Energy & Fuels* 1998;12:223-229.
- [9] Jin H, Okamoto T, Ishida M. Development of a Novel Chemical-Looping Combustion: Synthesis of a Looping Material with a Double Metal Oxide of CoO-NiO. *Energy & Fuels* 1998;12:1272-1277.
- [10] Jin H, Okamoto T, Ishida M. Development of a Novel Chemical-Looping Combustion: Synthesis of a Solid Looping Material of NiO/NiAl<sub>2</sub>O<sub>4</sub>. *Industrial and Engineering Chemistry Research* 1999;38:126-132.
- [11] Jin H, Ishida M. Reactivity study on novel hydrogen fueled chemical-looping combustion. *International Journal of Hydrogen Energy* 2001;26:889-894.

- [12] Jin H, Ishida M. Reactivity Study on Natural-Gas-Fueled Chemical Looping Combustion by a Fixed-Bed Reactor. *Industrial and Engineering Chemistry Research* 2002;41:4004-4007.
- [13] Ishida M, Yamamoto M, Ohba T. Experimental results of chemical-looping combustion with NiO/NiAl<sub>2</sub>O<sub>4</sub> particle circulation at 1200 °C. *Energy Conversion and Management* 2002;43:1469-1478.
- [14] Mattisson T, Lyngfelt A, Cho P. Possibility of Using Iron Oxide As an Oxygen Carrier for Combustion of Methane with Removal of CO<sub>2</sub> - Application of Chemical-Looping Combustion. 5th International Conference on Greenhouse Gas Control Technologies, Cairns, Australia, 2000. p. 205-210.
- [15] Mattisson T, Lyngfelt A, Cho P. The use of iron oxide as oxygen carrier in chemical-looping combustion of methane with inherent separation of CO<sub>2</sub>. *Fuel* 2001;80:1953-1962.
- [16] Mattisson T, Lyngfelt A. Capture of CO<sub>2</sub> Using Chemical-Looping Combustion. First Biennial Meeting of Scandinavian-Nordic Section of the Combustion Institute, Göteborg, 2001. p. 163-168.
- [17] Cho P, Mattisson T, Lyngfelt A. Reactivity of iron oxide with methane in a laboratory fluidized bed - application of chemical-looping combustion. 7th International Conference on Circulating Fluidized Beds, Niagara Falls, Ontario, 2002. p. 599-606.
- [18] Mattisson T, Järnäs A, Lyngfelt A. Reactivity of some metal oxide supported on alumina with alternating methane and oxygen - application for chemical-looping combustion. *Energy & Fuels* 2003;17:643-651.
- [19] Mattisson, T., Johansson, M., and Lyngfelt, A., "Multi-cycle reduction and oxidation of different types of iron oxide particles - application to chemical-looping combustion" *Energy & Fuels* 2004 (in press)
- [20] Cho, P., Mattisson, T. and Lyngfelt, A., "Comparison of iron-, nickel-, copper- and manganese-based oxygen carriers for chemical-looping combustion", *Fuel* 2004;83:1215-1225
- [21] Ryu H-J, Bae D-H, Han K-H, Lee S-Y, Jin G-T, Choi J-H. Oxidation and Reduction Characteristics of Oxygen Carrier Particles and Reaction Kinetics by Unreacted Core Model. *Korean Journal of Chemical Engineering* 2001;18(6):831-837.
- [22] Ryu H-J, Bae D-H, Jin G-T. Carbon Deposition Characteristics of NiO Based Oxygen Carriers Particles for Chemical-Looping Combustion. 6th International Conference on Greenhouse Gas Control Technologies, Kyoto, Japan, 2002.
- [23] Ryu H-J, Lim N-Y, Bae D-H, Jin G-T. Carbon Deposition Characteristics and Regenerative Ability of Oxygen Carrier Particles for Chemical-Looping Combustion. *Korean Journal of Chemical Engineering*

2003;20(1):157-162.

[24] Song K S, Seo Y S, Yoon H K, Cho S J, Characteristics of the NiO/Hexaaluminate for Chemical Looping Combustion, Korean Journal of Chemical Engineering 2003;20(3), 471-475.

[25] Ryu H-J, Bae D-H, Jin G-T. Effect of Temperature on Reduction Reactivity Oxygen Carrier Particle for Chemical-Looping Combustor in a Fixed Bed Reactor. Korean Journal of Chemical Engineering 2003;20(5):960-966.

[26] Ryu H-J, Bae D-H, Jin G-T. Chemical-Looping Combustion Process with Inherent CO<sub>2</sub> Separation; Reaction Kinetics of Oxygen Carrier Particles and 50 kWth Reactor Design, The World Congress of Korean and Korean Ethnic Scientists and Engineers-2002, Seoul, Korea, 738-743 (2002).

[27] Copeland RJ, Alptekin G, Cessario M, Gebhard S, Gerhanovich Y. A Novel CO<sub>2</sub> Separation System. The 8TH International Symposium on Transport Phenomena and Dynamics of Rotating Machinery, Honolulu, Hawaii, USA, 2000.

[28] Copeland RJ, Alptekin G, Cessario M, Gerhanovich Y. A Nobel CO<sub>2</sub> Separation System. First National Conference on Carbon Sequestration, National Energy Technology Laboratory (NETL), Washington, 2001.

[29] Copeland RJ, Alptekin G, Cessario M, Gerhanovich Y. Sorbent Energy Transfer System (SETS) for CO<sub>2</sub> Separation with High Efficiency. The 27th International Technical Conference on Coal Utilization & Fuel Systems, Clearwater, Florida, USA, 2002.

[30] Adanéz, J, de Diego, L F, García-Labiano F, Gayán P, Abad A, Placios J M, Selection of Oxygen Carriers for Chemical-Looping Combustion, Energy & Fuels 2004;18:371-377

[31] Hatanaka T, Matsuda S, Hatano H. A New-Concept Gas-Solid Combustion System "MERIT" for High Combustion Efficiency and Low Emissions. Intersociety Energy Conversion Engineering Conference, Honolulu, Hawaii, 1997. p. 944-948.

[32] Villa R, et al., Ni Based Mixed Oxide Materials for CH<sub>4</sub> Oxidation under Redox Cycle Conditions, Journal of Molecular Catalysis A: Chemical 2003; 204-105:637-646.

**Table 1. Composition of fuel and comparison to refinery gas.**

		Natural gas, %	Refinery gas, %
methane	CH <sub>4</sub>	88.09	68.16
ethane	C <sub>2</sub> H <sub>6</sub>	6.50	9.47
ethene	C <sub>2</sub> H <sub>4</sub>	0.00	0.02
propane	C <sub>3</sub> H <sub>8</sub>	2.70	7.46
propene	C <sub>3</sub> H <sub>6</sub>	-	0.01
isobutane	C <sub>4</sub> H <sub>10</sub>	0.38	1.08
n-butane	C <sub>4</sub> H <sub>10</sub>	0.56	3.14
n-pentane	C <sub>5</sub> H <sub>12</sub>	0.09	-
isopentane	C <sub>5</sub> H <sub>12</sub>	0.11	-
hexane	C <sub>6</sub> H <sub>14</sub>	0.05	-
hydrogen	H <sub>2</sub>	-	7.91
nitrogen	N <sub>2</sub>	0.34	0.75
carbon dioxide	CO <sub>2</sub>	1.18	2.02
hydrogen sulfide	H <sub>2</sub> S	0.00	0.08

**Table 2. Overview of tests with NiO-based oxygen-carrier. The last day, “demo”, involved demonstration of operation for the project participants.**

Day	hours
1	4.0
2	8.3
3	8.0
4	6.0
5	9.7
6	9.3
7	10.4
8	11.1
9	6.4
10	9.1
11	10.0
12	10.0
demo	3.3
total	107

**Table 3. Equilibrium concentrations of hydrogen and carbon monoxide.**

T, °C	800	850	900	950	1000
H <sub>2</sub> , %	0.40	0.42	0.45	0.48	0.51
CO, %	0.19	0.24	0.29	0.36	0.43
CO+H <sub>2</sub> , %	0.58	0.66	0.75	0.84	0.94
After condensation of H <sub>2</sub> O:					
H <sub>2</sub> , %	1.19	1.27	1.36	1.44	1.53
CO, %	0.56	0.71	0.88	1.07	1.28
CO+H <sub>2</sub> , %	1.75	1.98	2.24	2.51	2.81

**Table 4. Size distribution of originally added particles and particles retrieved in the filter after the air reactor.**

	Day 1	Day 2	Day 3	Day 4	D. 5	D. 6	D. 7	D. 8	D. 9	D. 10	D. 11	D. 12
	%	%	%	%	%	%	%	%	%	%	%	%
<45	30.9	7.8	0.5	1.4	0.7	0.9	0.4	0.4	0.4	0.7	0.2	0.2
45-63	15.4	6.8	2.5	2.3	1.2	1.6	0.5	0.7	0.5	0.6	0.3	0.3
63-90	17.6	20.5	6.2	10.6	7.6	6.7	6.7	5.6	7.1	4.4	4.2	2.7
90-125	30.3	53.7	70.3	61.6	62.4	70.6	75.1	68.2	63.9	67.8	74.3	69.5
125-150	3.7	8.1	15.6	16.5	19.0	16.3	11.5	15.5	17.1	18.7	14.1	17.6
150-180	1.7	2.4	3.8	5.9	7.4	2.4	4.5	7.4	8.4	5.9	5.1	7.1
180-212	0.4	0.6	1.0	1.4	1.5	1.3	1.1	2.0	2.1	1.6	1.5	2.2
>212	0.09	0.1	0.2	0.3	0.2	0.2	0.2	0.3	0.4	0.4	0.3	0.4
Total	100	100	100	100	100	100	100	100	100	100	100	100

**Table 5. Massbalance for the whole test period. The numbers are given in relation to the initially added mass.**

elutriated from air reactor	73.1%
elutriated from fuel reactor	4.5%
leaks	3.9%
total lost	81.5%
initially added	100.0%
recycled day 6+10	32.3%
initially added + recycled - lost	50.8%
remaining	48.9%
balance	-1.9%

**Table 6. Particle costs**

particle inventory <sup>1</sup>	0.1-0.2	ton/MW
lifetime <sup>2</sup>	4 000	h
specific particle cost <sup>3</sup>	4	€/kg
specific emission	0.2	ton CO <sub>2</sub> /MWh
resulting particle cost	0.5-1	€/ton CO <sub>2</sub> captured

<sup>1</sup> Somewhat uncertain value, but without doubt in the correct order of magnitude.

<sup>2</sup> Conservative assumption. Loss of fine material in prototype tests suggests a lifetime that is 10 times longer, i.e. 40 000 h.

<sup>3</sup> The particle cost is estimated to 4 €/ton. If fine material lost in the process can be used as raw material in the production, the costs can be decreased significantly, but not below the production cost 1 €/ton.



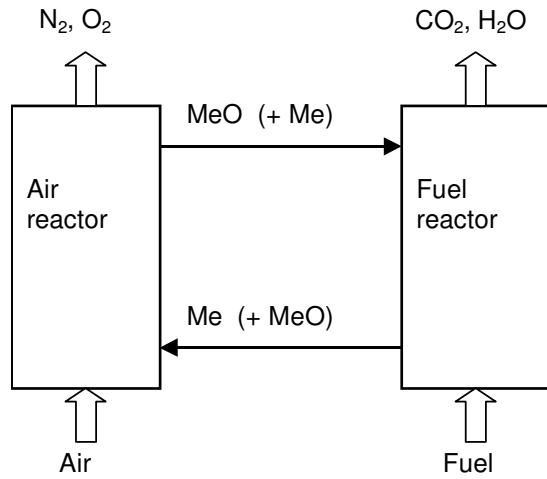


Fig. 1. Chemical-looping combustion. MeO/Me denote recirculated oxygen carrier solid material.

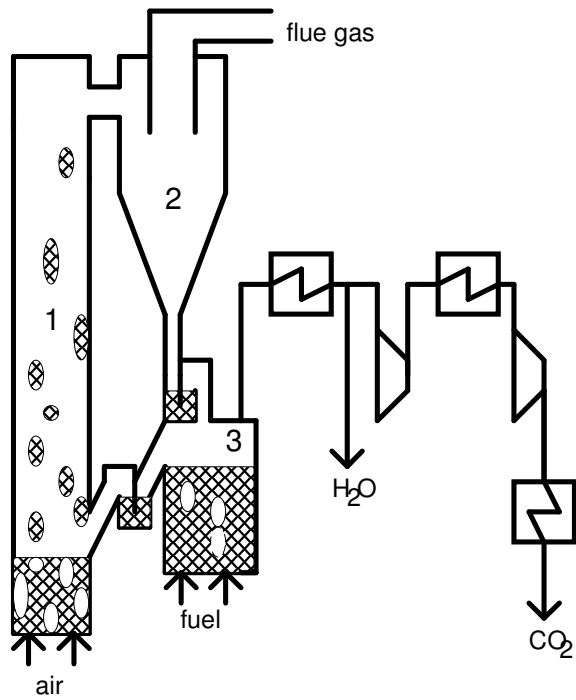


Fig. 2. Layout of chemical-looping combustion process, with two interconnected fluidized beds. 1) air reactor, 2) cyclone, 3) fuel reactor.

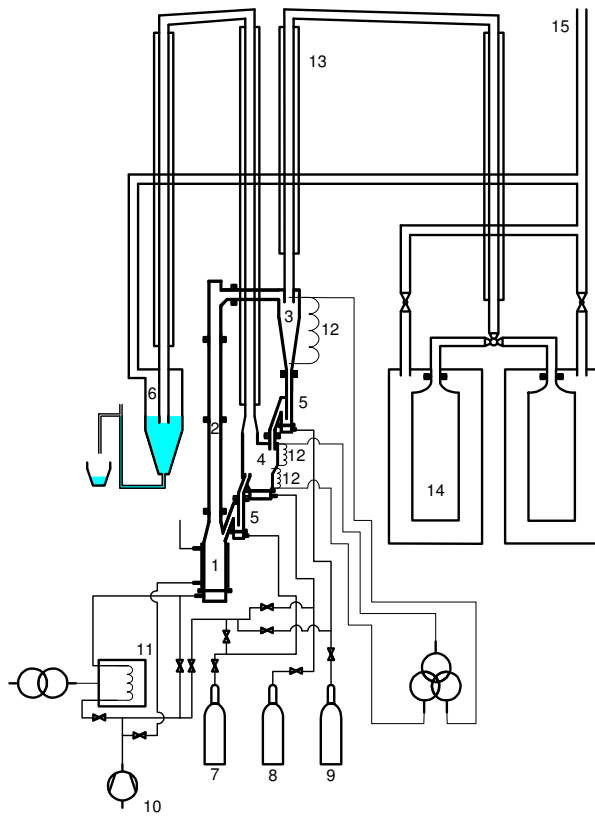


Fig. 3. Drawing of prototype reactor system, also indicating the cooling and particle separation systems.

1) air reactor, 2) riser, 3) cyclone, 4) fuel reactor, 5) upper and lower particle locks, 6) water trap, 7) nitrogen 8) natural gas, 9) argon, 10) air, 11) preheater, 12) heating coils (not available for tests with nickel-based particles), 13) finned tubes for cooling of gas streams, 14) filters and 15) connection to chimney.

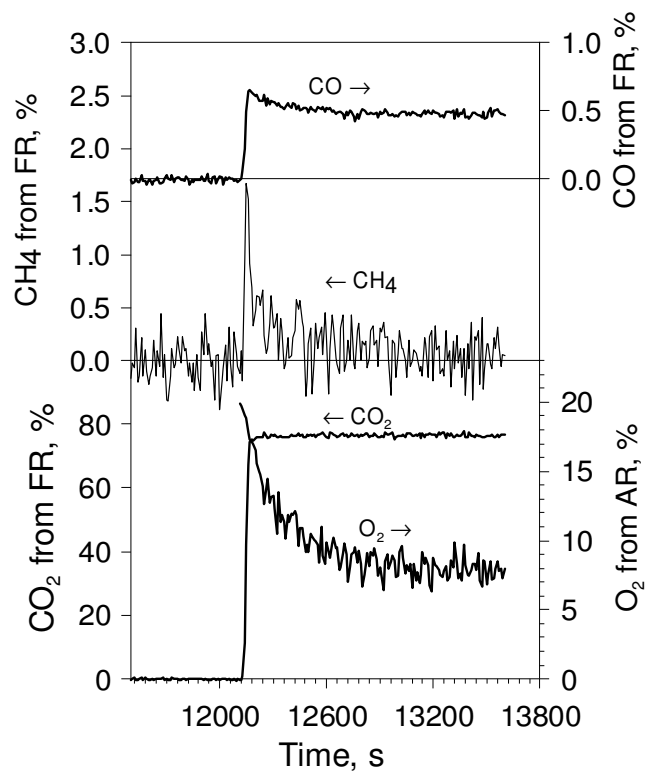


Figure 4. Start of operation.

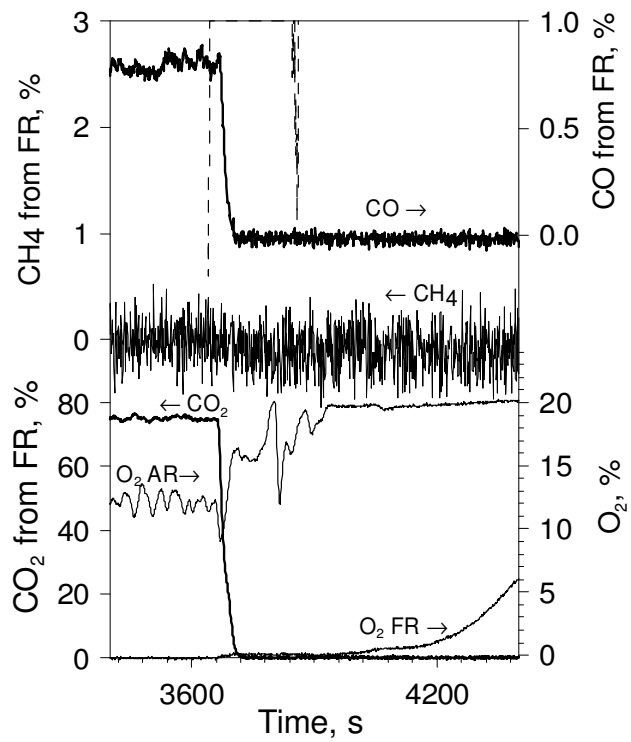


Figure 5. Stop of fuel.

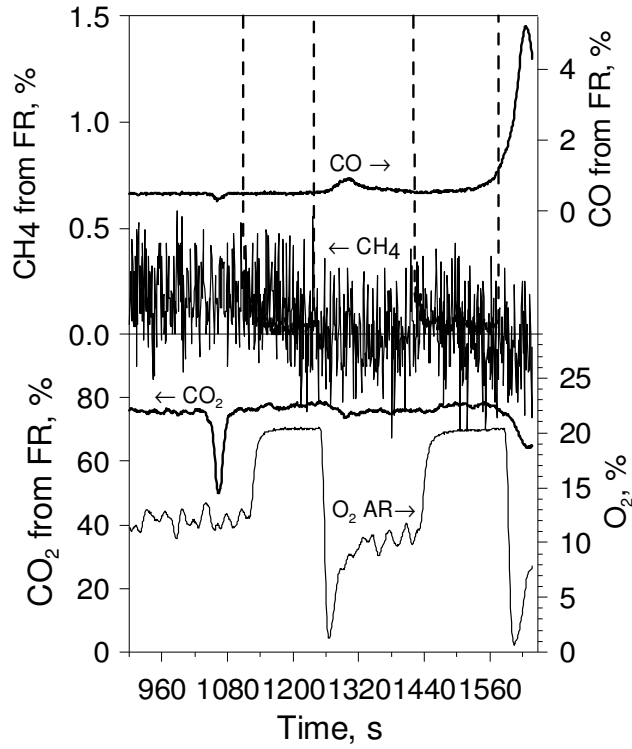


Figure 6. Stop of circulation. Vertical, dashed lines show stop and start of fluidization of lower particle lock. (The fluctuation in CO<sub>2</sub> and CO at 1040 s is caused by rinsing of the pressure taps.)

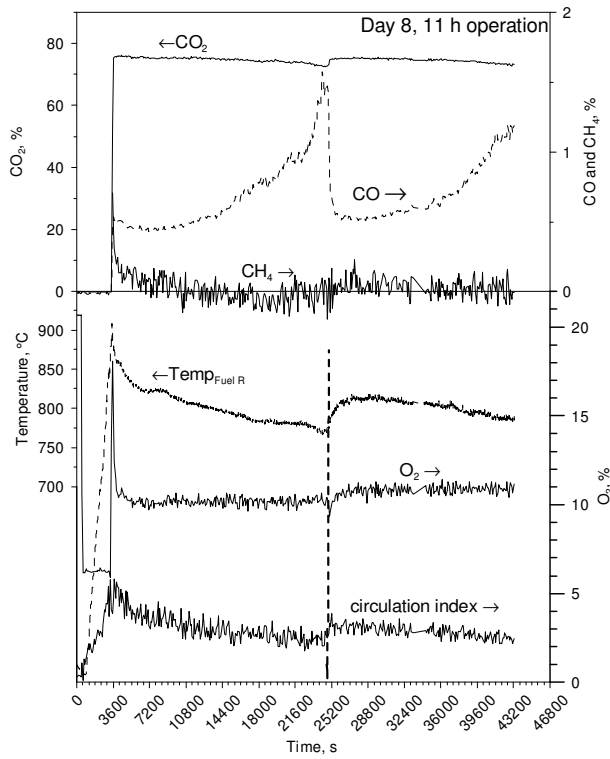


Figure 7. Example of 11 hours of operation from day 8. Vertical, dashed line shows increase in air flow.

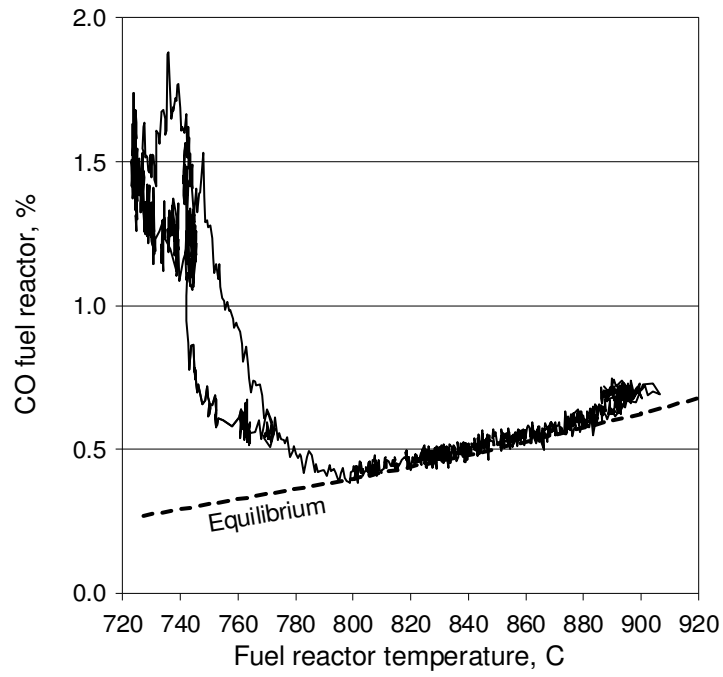


Figure 8. CO versus fuel reactor temperature.

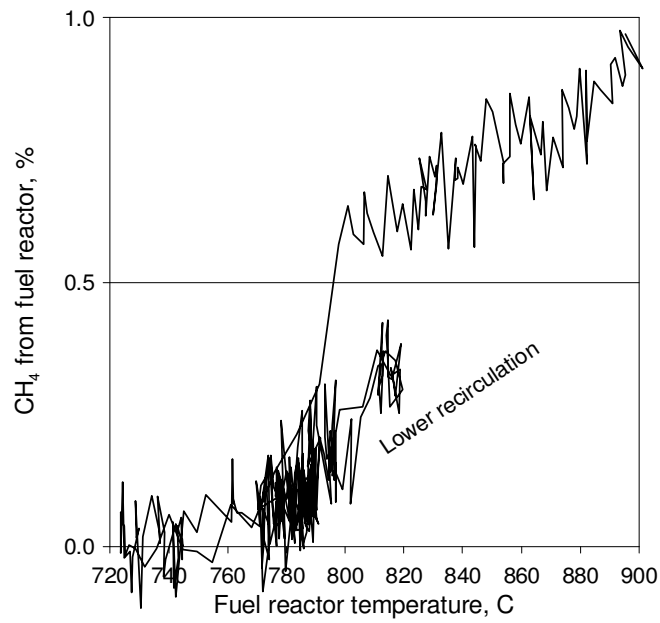


Figure 9. CH<sub>4</sub> versus fuel reactor temperature.

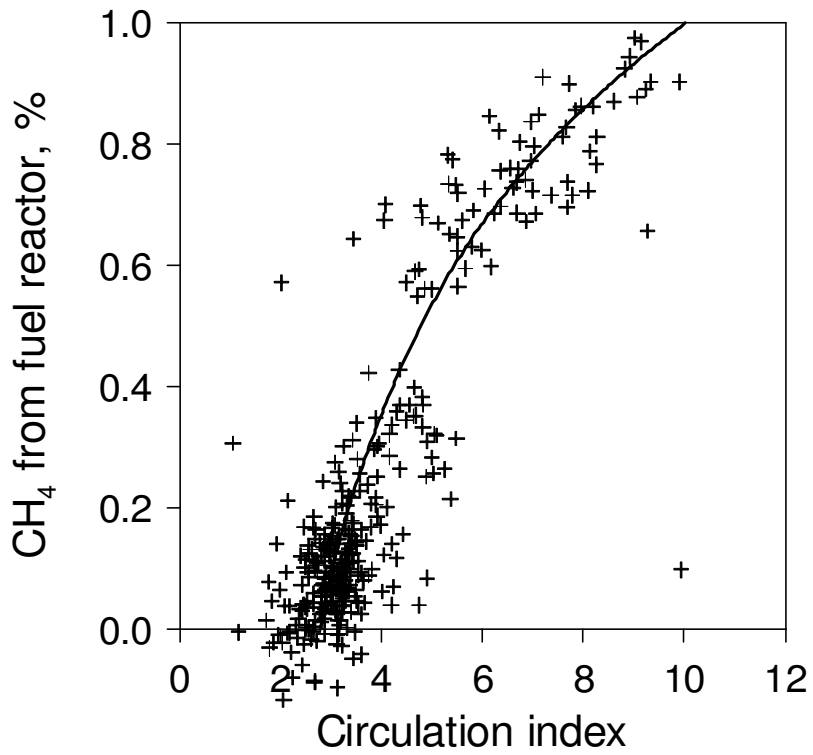


Figure 10. CH<sub>4</sub> versus estimated circulation.

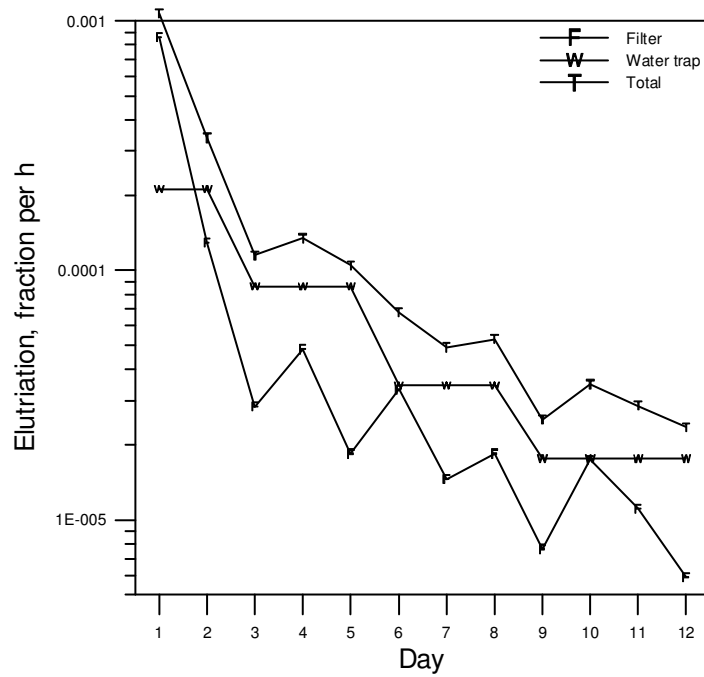


Figure 11. Fractional loss of fines vs time. Time of recirculation includes period with no reaction.

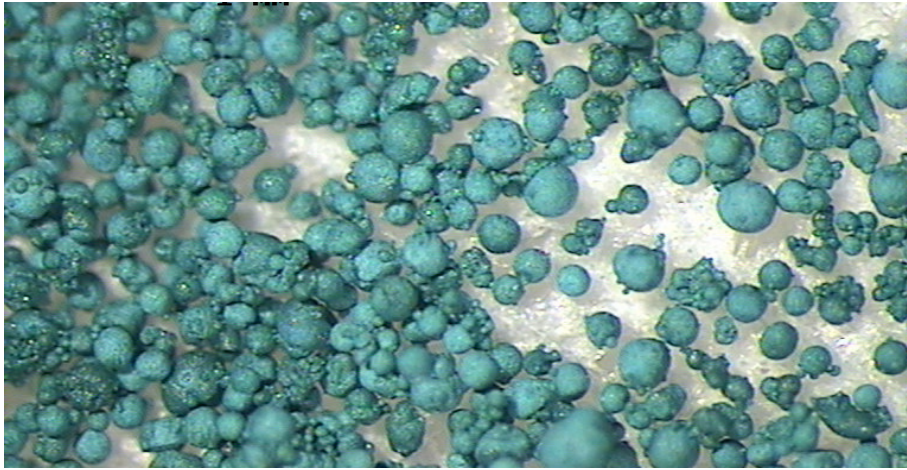


Figure 12. Photo of material added to the prototype. There is fine material in the form smaller spherical "satellites" which is sintered onto the surface of the larger particles.

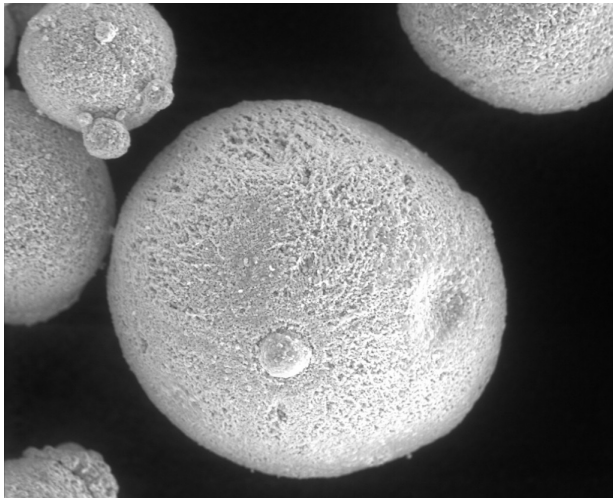


Figure 13. SEM photo of particles in Fig. 12.

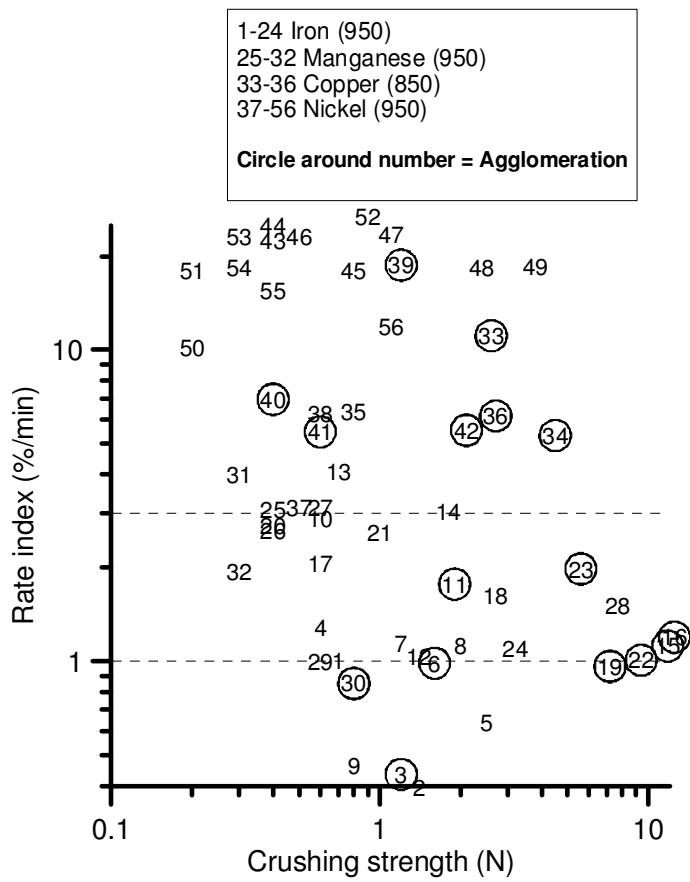


Fig. 14. Rate index versus crushing strength for particles produced by freeze-granulation.